A RHO GTPase-mediated pathway is required during P cell migration in *Caenorhabditis elegans*

Andrew G. Spencer*†, Satoshi Orita*†‡, Christian J. Malone*†§, and Min Han†¶

†Howard Hughes Medical Institute, Department of Molecular Cell and Developmental Biology, University of Colorado, Boulder, CO 80309-0347; and ‡Shionogi and Co., Osaka 553-0002 Japan

Communicated by William B. Wood, University of Colorado, Boulder, CO, September 24, 2001 (received for review August 26, 2001)

The Rho family of guanine triphosphate hydrolases controls various cellular processes, including cell migration. We describe here the demonstration of a role for a RhoA GTPase homologue during cell migration in *Caenorhabditis elegans.* We show that eliminating or reducing *rho-1* gene function by using a dominant-negative transgene or dsRNA interference results in a severe defect in migration of hypodermal P cells to a ventral position. Biochemical and genetic data also suggest that *unc-73*, which encodes a Trio-like guanine nucleotide exchange factor, may act as an activator of *rho-1* in the migration process. Mutations in *let-502* ROCK, a homologue of a RhoA effector in mammals, also cause defects in P cell migration, suggesting that it may be one of several effectors acting downstream of *rho-1* during P cell migration. Finally, we provide evidence to support the idea that other small Rac subfamily small GTPases act redundantly and in parallel to RHO-1 in this specific cell migration event.

rho-1 | *rac* | *unc-73*

The Rho family of small GTPases, including the Rho, Rac, and Cdc42 subfamilies, are key regulators of the actin cytoskeleton. During a variety of cellular events, including polarization, shape reorganization, and migration, Rho GTPases serve to transduce signals between extracellular ligands and cytoskeletal reorganization (1). These switch proteins cycle between an inactive GDP-bound form and an active GTP-bound form. The active state of Rho proteins is directly regulated by guanine nucleotide exchange factors (GEFs), which catalyze the release of GDP and thereby facilitate GTP binding and subsequent activation. In mammalian cells and other systems, activated Rho family members have demonstrated roles in cytoskeleton reorganization, with distinct reorganization patterns for each subfamily member. For example, in Swiss 3T3 cells, overexpression of Rho, Rac, or Cdc42 results in the assembly and organization of stress fibers, lamellipodia, or filopodia, respectively (2). How the various Rho family GTPases are spatially and temporally regulated during developmental morphogenesis is not well understood.

Rho-1 is known to be required for early events in *Drosophila* development, such as dorsal closure and gastrulation (3, 4). In addition, the Rho GEF Pebble is specifically required for cytokinesis (5). Another *Drosophila* GEF, Trio, was recently shown to regulate the Rho family effector Pak through the GTPase Rac during axon guidance (6). Mutations in the *Caenorhabditis elegans* Trio homologue, *unc-73*, also cause defects in cell migration and axon guidance (7). Both Trio and *unc-73* contain two GEF domains, each of which contains successive Dbl homology (DH) and pleckstrin homology (PH) domains. In the case of Trio, the two GEF domains have been shown to specifically activate different Rho GTPases (8, 9).

Studies of mutant alleles of *unc-73* have led to the hypothesis that *unc-73* is generally required for cell migrations in *C. elegans* and can regulate the activity of Rac (7). Potential targets of *unc-73* include *mig-2* and *ced-10/rac-1*, which encode proteins similar to mammalian Rac proteins, as the roles of these two GTPases in cell migration and axon guidance have been reported previously (10, 11).

The experiments described in this report examine the molecular basis of a cell migration event during *C. elegans* larval development. P cells are present on the sublateral surface of the *C. elegans* larvae on hatching (12). During mid-L1, the P cells are loosened from neighboring cells, and their leading edges begin to intercalate along the ventral cord as the leading edge of cytoplasm moves to a ventral contralateral position (13). Soon afterward, P cell nuclei move ventrally and come to rest at the ventral midline. Once migration is complete, each P cell divides to generate five neurons and one hypodermal cell in the *C. elegans* hermaphrodite. Descendants from three of these P cells are later induced to form the hermaphrodite vulva. We look specifically at the role of *rho-1* in the P cells and provide evidence that *rho-1* is required for their ventral migration.

Materials and Methods

Site-Directed Mutagenesis. Mutagenesis was performed by using the Stratagene QuickChange kit. Primers (Operon Technologies, Alameda, CA, or GIBCO) were designed to make two mutations in *C. elegans rho-1* and *ced-10/rac-1. rho-1* T19N (dominant negative) and *rho-1* G14V (constitutively active or gain of function) are referred to here as *rho-1(dn)* and *rho-1(gf)*, respectively. Mutant cDNAs were cloned into multiple cloning site (MCS)II of the *col-10* promoter (V. Ambros, personal communication) vector by using the *Nhe*I(5′) and *Sac*I(3′) restriction sites. A cDNA encoding the Rho toxin C3 from *Clostridium botulinum* was obtained by PCR and inserted into the *col-10* promoter vector by using *Kpn*I sites.

The *col-10* Promoter Vector. The *col-10* promoter vector was constructed from plasmid pPD49.26 containing two MCS and the 3′ untranslated region of *unc-54* (gift from A. Fire, Carnegie Institute). Into MCSI, we cloned a 1.17-kb region of genomic DNA upstream of the *col-10* translational start site by using *Xba*I (5′) and *Bam*HI (3′). cDNAs of interest [C3, *rho-1(dn)*, *rho-1(gf)*, *rac-1(dn)*] were then cloned into MCSII by using *Nhe*I (5′) and *Sac*I (3′).

The *unc-73*(+) minigene (7) was a gift from R. Steven and J. Culotti (University of Toronto, Toronto, ON). To establish transgenic lines, 10 ng/μl of *unc-73*(+) was injected along with 90 ng/μl of *sur-5*:*GFP* cDNA into *unc-73(e936)* animals. The *sur-5*::*GFP* was used as an injection marker and results in green fluorescent protein (GFP) expression in all somatic cell nuclei

Abbreviations: GEF, guanine nucleotide exchange factor; DH, Dbl homology; PH, pleckstrin homology; MCS, multiple cloning site; GFP, green fluorescent protein; dsRNA, double-stranded RNA; DAPI, 4′,6-diamidino-2-phenylindole.

*A.G.S., S.O., and C.J.M. contributed equally to this work.

§Present address: 227D R.M. Bock Labs, University of Wisconsin, Madison, WI 53706.

¶To whom reprint requests should be addressed. E-mail: mhan@coloradoedu.

The publication costs of this article were defrayed in part by page charge payment. This article must therefore be hereby marked "*advertisement*" in accordance with 18 U.S.C. §1734 solely to indicate this fact.

www.pnas.org/cgi/doi/10.1073/pnas.241504098

(14). Several stable lines expressing the array were established, all of which were rescued for the *unc-73(e936)* P cell phenotype.

Strains and Matings. The wild-type strain used was N2 Bristol. The following strains were also used: *let-502(sb106)* (15), *let-502(h392)*, and *mel-11(it26)* (16); *mig-2(mu28, null)*; *mig-2(gm103, gf)* (10); *unc-73(e936)*; *unc-73(rh40)* (7, 17); and *dpy-5/unc-73(gm40)* and *unc-47*::*GFP* integrated line (18). Other strains were obtained from the Caenorhabditis Genetics Center at the University of Minnesota.

The *rho-1(dn)* transgenic lines were made by injecting *dpy-20 (e1282); unc-47*::*GFP* animals with 10 ng/μl of *rho-1(dn)* cDNA in the *col-10* promoter vector and 25 ng/μl of rescuing *dpy-20*(+) DNA. Animals propagating this simple array were therefore *dpy-20(e1282)*; *unc-47*::*GFP*; *kuEx130*[*col-10*:*rho-1(dn)*; *dpy-20*(+)]. The extrachromosomal array was integrated into the chromosome by using γ irradiation as described previously (19) to give *dpy-20(e1282)*; *unc-47*::*GFP*; *kuIs52*[*col-10*:*rho-1(dn)*; *dpy-20*(+)]. We refer to this strain simply as *rho-1(dn)*. Six stable integrated lines were established, all of which displayed a phenotype similar to each other and to the *rho-1(dn)* line expressing the extrachromosomal array. Transgenic lines expressing a *rho-1*(G14V, *gf*) transgene under control of the *col-10* promoter were established by injecting the N2 strain with 10 ng/μl of *rho-1(gf)* cDNA in the *col-10* promoter vector and 90 ng/μl of *sur-5*:*GFP* cDNA.

We made the *mig-2(mu28)*; *unc-73(e936)* double mutant as follows. Males homozygous for the null *mig-2 (mu28)* allele, which is on the X chromosome, were crossed into *unc-73(e936)*; *dpy-6(e14)* hermaphrodites (*dpy-6* maps four map units from *mig-2*). *unc-73* F2 progeny were obtained, and those animals unable to throw Dpy progeny were *mig-2(mu28)*; *unc-73(e936)* double mutants. The Unc phenotype was severely exacerbated compared with that observed in *unc-73(e936)*.

RNAi of *let-50, mig-2,* and *rho-1*. RNAi results in the inactivation of a gene corresponding to injected double-stranded (ds)RNA sequences and was performed essentially as described by Fire *et al.* (20). For *let-502*, PCR primers were designed to amplify a 2.9-kb region of a *let-502* cDNA provided by Paul Mains (University of Calgary; ref. 16). For *mig-2*, T7/T3 flanked PCR primers were designed to amplify a ≈600-bp piece of genomic *mig-2* DNA, including most of exon 2. dsRNAi corresponding to *mig-2* sequences was injected into homozygous *ced-10/rac-1(n3246)* animals. After 24–48 h, F1 progeny were scored for P cell migration in the second larval stage. For *rho-1*, primers were designed to amplify nearly all of a 625-nt cDNA. P cell migration success was scored (see below) in *let-502(RNAi)* larvae 24–36 h after injection of mothers. To score P cell migration success in *rho-1(RNAi)* escapers, animals injected with dsRNA were moved to individual plates 5 h after injections. The next day, nonwild-type (Unc, lumpy) larvae present on plates containing arrested embryos were observed under Nomarski optics and scored as described below.

Scoring P Cell Migration Success. To score P cell migration success, animals were picked during L2 and observed under Nomarski optics. Ventral to the nerve cord, P1.p through P11.p nuclei were counted manually in the wild-type N2 strain, mutant, and transgenic animals. That defects were caused by cell migration was confirmed by observation of ectopic lateral neurons. When fewer than 11 Pn.p cells were observed, we checked the lateral surface for, and typically found, ectopically differentiated neurons. To score *let-502(sb106)* animals for P cell migrations, mothers kept at the permissive temperature (15°C) were shifted to 25°C and allowed to lay eggs for 3 h. Mothers were then removed, and the larvae were scored the next day at the L2 stage. To confirm P cell migration defects in various mutant and transgenic backgrounds, we crossed or injected into a strain containing an integrated copy of an *unc-47*::*GFP* transgene (18). In this strain, UNC-47::GFP is expressed in 26 GABA neurons, including 13 P cell-derived neurons present in the ventral cord in wild-type animals.

Table 1. P cell migration defects in *rho-1* and *unc-73* strains

Genotype	No. of Pn.p cells migrated†	*n*
N2	11.0 ± 0.0	25
Ex col-10:rho-1(T17N, dn)	3.4 ± 1.0	25
Is col-10:rho-1(T17N, dn)	3.1 ± 0.7	25
col-10:C3	5.9 ± 1.4	25
rho-1(RNAi) escapers	5.2 ± 1.7	22
unc-73(gm40)	7.1 ± 1.2	28
unc-73(e936)	7.6 ± 1.1*	25
Ex rho-1(G14V, gf)	11.0 ± 0.0	25
unc-73(e936);Ex rho-1(G14Vgf)	9.8 ± 0.7*	25
unc-73(rh40)	10.8 ± 0.4	25

Pn.p cells were scored during the L2 stage, as described in *Materials and Methods*. Ex, Exchromosomal array; Is, Integrated line. ±, SD.
*, *P* value is <0.0001 when these data are compared by using Student's *t* test.
†Data are expressed as the average number of Pn.p cells in the ventral cord during L2.

GDP/GTP Exchange Assays. We refer to the DH1/PH1 and DH2/PH2 domains of UNC-73 (7) as GEF1 and GEF2, respectively. The UNC-73 GEF1 and GEF2 proteins used for exchange assays were produced in HeLa cells by using pSO19 and pSO20, as described (21). Briefly, HeLa cells were plated at a density of 5×10^6 cells/100-mm dish and were incubated for 18 h. HeLa cells were infected with T7 RNA polymerase recombinant vaccinia virus (LO-T7) (gift from Michinori Kohara, Tokyo Metropolitan Institute of Medical Science) and then transfected with 15 mg of pSO19, pSO20 or pGEM-HA. After transfection, cells were resuspended in 0.2 ml of ice-cold suspension buffer (25 mM Tris·HCl at pH 7.5/1 mM DTT/0.5 mM EDTA). The lysates were prepared by using a Dounce homogenizer, and insoluble materials were removed by centrifugation in a microcentrifuge for 15 min at 4°C. RhoA and Rac1 were purified from baculovirus-infected cells (provided by Yoshimi Takai, Osaka University) (22). Exchange assays were performed by using 30 μl of HeLa cell lysates and 2 pmol of [^{3}H]-GDP-bound form of each small GTP-binding protein, as described (22).

Results

***rho-1* Activity Is Required for P Cell Migration in *C. elegans*.** Analysis by using RNA interference indicates that the eliminating the *rho-1* gene activity disrupts embryogenesis with arrested embryos, showing defects in cytokinesis (data not shown; ref. 23). To circumvent the lethality caused by *rho-1(RNAi)* and explore the role of *rho-1* during the migration of P cells, we expressed a dominant-negative version of *rho-1*, *rho-1*(T19N) (see *Discussion*), under control of the *col-10* promoter. The *col-10* transcript is enriched during larval stages in hypodermal lineages (V. Ambros, personal communication), which include P cells. Expression of the *col-10*-driven *rho-1(dn)* from an extrachromosomal array resulted in a severe P cell migration defect (Table 1). Integration of the array into the genome had a similar and slightly stronger effect (Table 1). The P cell migration defect in *rho-1(dn)* animals was evident because of the lack of Pn.p cells in the ventral cord during the L2 stage (compare Fig. 1 *A* and *B*). In addition, we observed ectopic P cell-derived neurons on the lateral surface of *rho-1(dn)* animals, indicating that P cells were able to divide and differentiate somewhat normally in the absence of migration (Fig. 1*C*). The presence of ectopic neurons indicates that the *rho-1(dn)*-induced defect is caused by failed

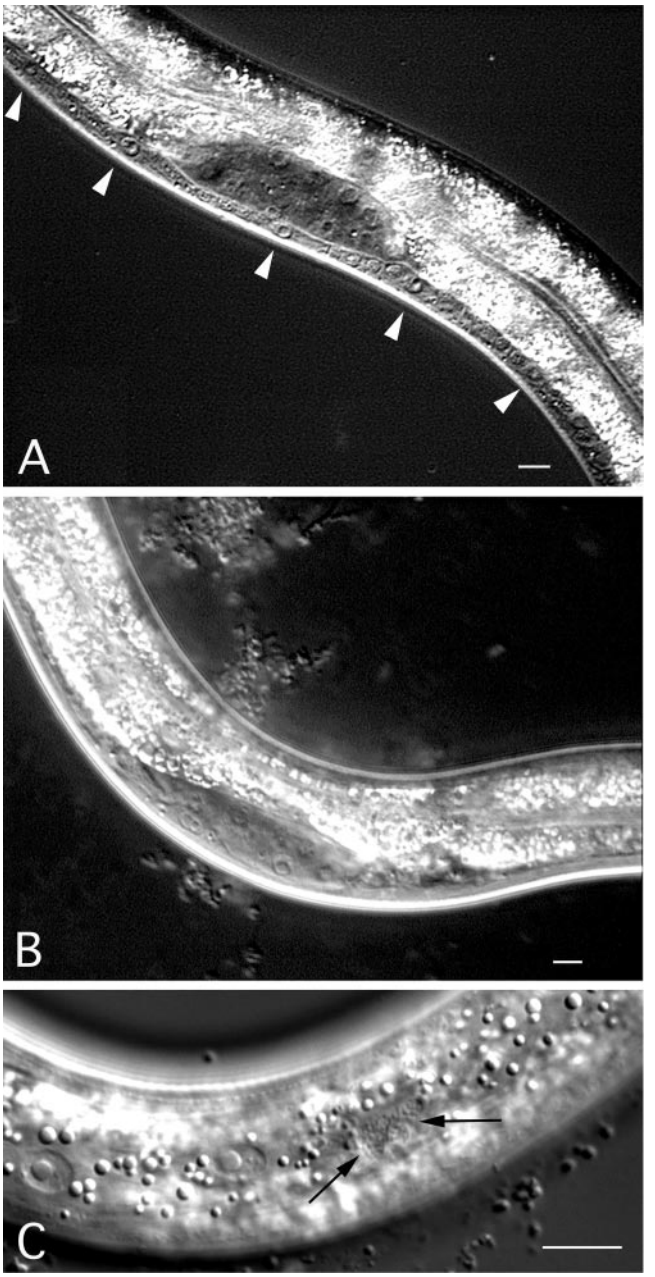

Fig. 1. Phenotype of rho-1(dn) animals. (*A*) Bristol N2 strain during the second larval stage with P cells (arrowheads) and a full ventral cord; (*B*) *rho-1(dn)* animals lacking P cells and many descendants thereof in the ventral cord. The ventral cord is very thin in this animal because of missing P cells. (*C*) Lateral surface of a *rho-1(dn)* animal during L2 animal showing ectopic P cell neuronal descendants (arrows). (Bar = 10 μm.)

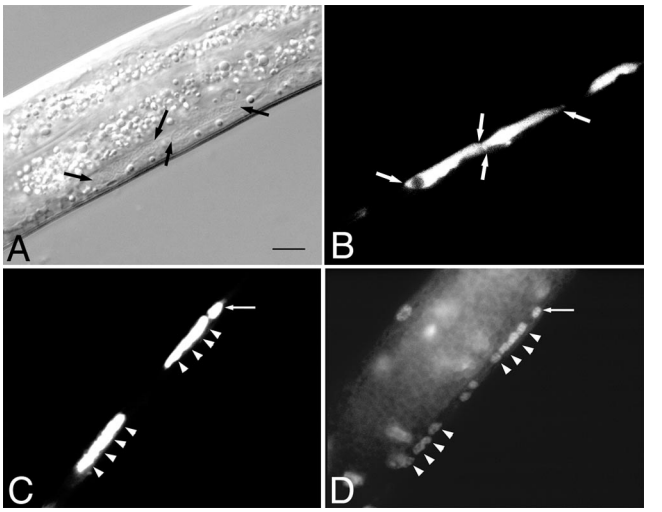

Fig. 2. *rho-1(dn)* can cause a cytokinesis defect. (*A*) Abnormally large neurons (flanked by arrows) in a living *rho-1(dn)* animal during the second larval stage. (*B*) Fluorescent visualization of the *unc-47*::*GFP*-positive cells (flanked by arrows) in the animal shown in *A*. (*C*) Fluorescent visualization of *unc-47*::*GFP*-positive neurons in a fixed *rho-1(dn)* animal. (*D*) DAPI visualization of the multiple nuclei observed in the *unc-47*::*GFP*-positive cells shown in *C*. Arrowheads in *C* and *D* denote the positions of nuclei as determined by DAPI staining. Arrows in *C* and *D* show an *unc-47*::*GFP*-positive cell without the cytokinesis defect. (Bar = 7 μm.) In wild-type animals (see Fig. 1*A*), multiple neurons are clearly visible in the same region of a multinuclear cell in the mutant.

cell migration and not by a transformation of cell fate or nuclear migration defect, which leads to cell death (24, 25). These ectopic neurons are sometimes difficult to find but can be identified in ≈60% of *rho-1(dn)* animals.

The *rho-1(dn)*-induced P cell migration defect resulted in Vulvaless animals unable to lay eggs (data not shown) or mate efficiently. In addition, *rho-1(dn)* expression caused severe uncoordination because of mislocalization and changes in the morphology of neurons normally found in the ventral cord. In *rho-1(dn)* animals, several ventral cord neurons, including some GABA neurons, which are marked by an *unc-47*::*GFP* transgene (18), assume a long extended shape and appear to be significantly larger than their wild-type counterparts (Fig. 2 *A* and *B*). Staining of *rho-1(dn)* animals with the DNA dye 4′,6-diamidino-2-phenylindole (DAPI) revealed many, but not all, of these cells to be multinucleate (Fig. 2 *C* and *D*), suggesting *rho-1(dn)* can cause a cytokinesis defect in these cells (23).

We used two methods to test the hypothesis that the *rho-1(dn)* transgene specifically reduced *rho-1*(+) activity, as opposed to interfering with other Rho family GTPases. First, we expressed the *C. botulinum* toxin C3 from the *col-10* promoter. C3 ADP-ribosylates and specifically inactivates *rho-1*; it appears to have no toxic effect on other Rho family proteins like Rac and Cdc-42 (26). Expression of *col-10*:C3 in a wild-type background caused a severe P cell migration defect (Table 1). Secondly, we showed that reducing *rho-1*(+) activity by using RNAi results in failed P cell migrations. Injection of dsRNA corresponding to *rho-1* sequences caused embryonic arrest, as reported above. However, a small percentage of early progeny from *rho-1* dsRNA-injected hermaphrodites escaped the embryonic lethal phenotype and developed as uncoordinated kinky larvae. This effect is because of maternal rescue of the RNAi effect in the more proximal oocytes of dsRNA-injected hermaphrodites (27, 28). We scored P cell migration success in these *rho-1(RNAi)* escapers and found moderate to severe P cell migration defects similar to those observed in *col-10*::C3 transgenic animals (Table 1). When *rho-1(RNAi)* escapers were examined in the *unc-47*::*GFP* background, we again observed the P cell migration defect. In addition, we saw a reduction in the number and changes in the morphology of GABA neurons in the ventral cord similar to the phenotype seen in *rho-1(dn)* animals (data not shown; Fig. 2 *A* and *B*). The *rho-1(RNAi)* escapers grew to adulthood but were sterile because of defective gonad development. The combined results of C3 expression and *rho-1(RNAi)* escapers indicate clearly that *rho-1*(+) activity is required for P cell migration.

***unc-73* May Act as an Exchange Factor for *rho-1* During P Cell Migration.** GEFs catalyze the release of GDP from RHO-1 to facilitate GTP binding and RHO-1 activation. Mutations in

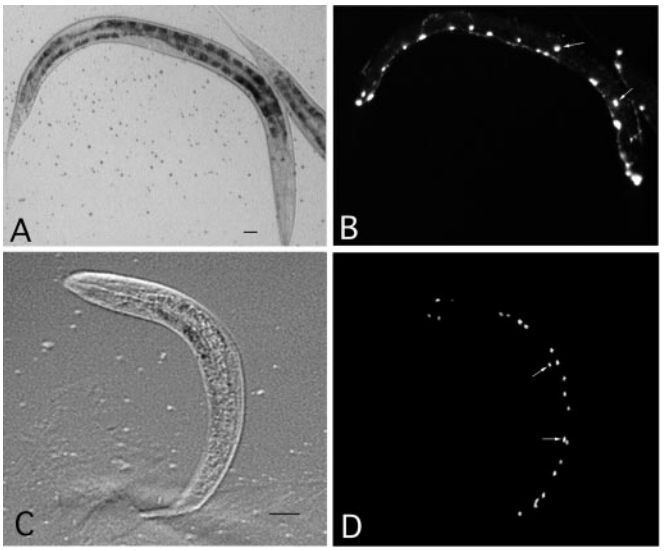

Fig. 3. *unc-47*::*GFP* visualization of P cell-derived neurons in strains with P cell migration defects. (*A*) Nomarski and (*B*) fluorescent image of *unc-73(e936)* in the *unc-47*::*GFP* background. (*C*) Nomarski and (*D*) fluorescent image of a *let-502(RNAi)* larva in the *unc-47*::*GFP* background. Mislocalized GABA neurons are indicated with white arrows.

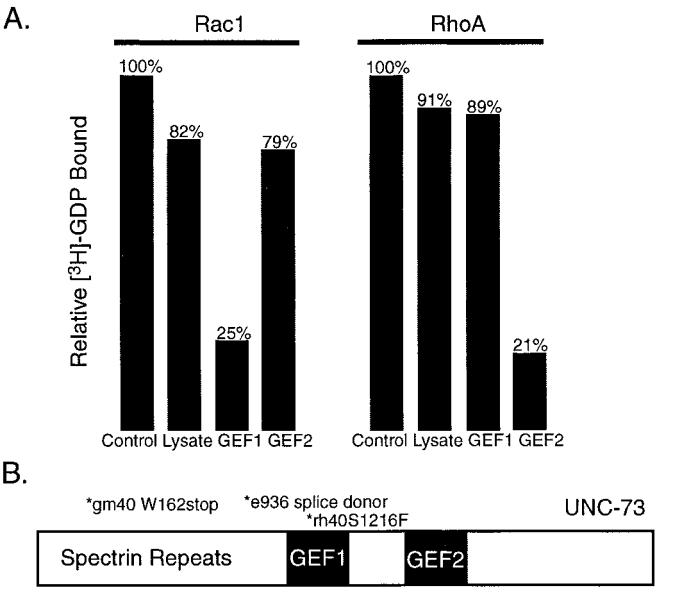

Fig. 4. GDP/GTP exchange assays. HeLa cell extracts expressing GEF1 or GEF2 of UNC-73 were assayed for their ability to catalyze GDP release from RhoA and Rac1, as described in *Materials and Methods*. (*A*) Relative amounts of bound [^{3}H]-GDP after incubation of GEF1 or GEF2 with Rac1 or RhoA. (*B*) Schematic diagram of UNC-73.

unc-73 cause axon guidance defects and failed migrations in some cell types, including P cells (7, 29–31). We show here that two *unc-73* alleles, *gm40* and *e936*, cause similar partial P cell migration defects (Table 1). These P cell migration defects are observed in nearly all *unc-73* mutant animals, each showing a few affected cells. *gm40* and *e936* were previously characterized as putative null and partial loss-of-function mutation, respectively (7). *unc-73(e936)* and *unc-73(gm40)* display a similar penetrance of the cell migration phenotype. Because *gm40* homozygous animals are very unhealthy due to severe but incomplete embryonic and larval lethality, they are very difficult to score for migration analysis; therefore, we used *e936* for further study. To easily monitor the success of P cell migrations toward the ventral cord, we examined *unc-73(e936)* animals in the *unc-47*::*GFP* background (ref. 18; see *Materials and Methods*). In *unc-73(e936); unc-47*::*GFP* animals, some P cell-derived GABA neurons normally found in the ventral cord were observed on the lateral surface of animals during the second larval stage (Fig. 3 *A* and *B*). This observation confirms that some P cells fail to migrate ventrally and continue to differentiate in an ectopic position in *unc-73(e936)* animals. The P cell defect of *unc-73(e936)* animals was partially rescued by the *col-10* promoter-driven expression of *rho-1(gf)* (Table 1). Although the non-null nature of the *unc-73(e936)* allele makes such genetic interaction open to other interpretations, this result is consistent with *rho-1* acting downstream of *unc-73*. The *rho-1(gf)* transgene alone displayed normal P cell migrations.

We sought biochemical evidence that UNC-73 could act as an exchange factor for RHO-1. The exchange activities of GEFs are conferred by consecutive DH/PH domains (1, 32). Two such DH/PH domains are present in UNC-73 (Fig. 4*B*; ref. 7) and are referred to here as GEF1 and GEF2. Previously, an UNC-73 fusion protein containing only GEF1 was shown to exhibit exchange activity toward mammalian RAC1 (7). To directly determine whether either of the UNC-73 GEFs could catalyze GDP exchange from RHO, we expressed the GEF1 and GEF2 domains of UNC-73 separately in HeLa cells and measured their ability to catalyze the release of [^{3}H]-GDP from mammalian RHOA and RAC1. UNC-73 GEF1 was able to efficiently release [^{3}H]-GDP from RAC1 but not from RHOA (Fig. 4*A*). In contrast, UNC-73 GEF2 exhibited significant exchange activity only toward RHOA (Fig. 4*A*). These results indicate that GEF1 and GEF2 act specifically on RAC and RHO, respectively, *in vitro*. Given the high degree of homology between RHOA and *C. elegans* RHO-1 protein (see *Discussion*), it is reasonable to suggest that the UNC-73 GEF2 domain has the exchange activity on RHO-1 *in vivo*.

The *unc-73(rh40)* allele contains a missense mutation in GEF1 that eliminates its exchange activity (7). *unc-73(rh40)* mutants exhibit no significant P cell migration defect (Table 1, Fig. 4*B*), consistent with the possibility that GEF2 alone can activate RHO-1. However, there is no solid *in vivo* evidence to support a model that GEF1 and GEF2 of UNC-73 act specifically on Rac and Rho subfamily proteins, respectively, in *C. elegans*.

***let-502* ROCK Activity Is Required for P Cell Migration.** *let-502* encodes a Rho-kinase, and existing mutations in this gene result in larval arrest and elongation failure (16). In an attempt to identify downstream effectors of *rho-1* during P cell migration, we characterized the P cell migration success rate of several *let-502*-deficient animals. A strong loss-of-function allele of *let-502(h392)* exhibits a weak but reproducible P cell defect, and a similar P cell phenotype was also observed in a temperature-sensitive hypomorphic allele, *let-502(sb106)* (Table 2). Further, *let-502(RNAi)* causes an embryonic elongation phenotype similar to the *h392* allele and exhibits a comparable P cell migration defect (Table 2). When *let-502(RNAi)* was performed in the *unc-47*::*GFP* background, GABA neurons normally found ventrally were observed on the lateral surface of affected animals during the second larval stage (Fig. 3 *C* and *D*). Taken together, these observations suggest that *let-502* activity is required for wild-type P cell migration. Consistent with *let-502* acting downstream of *rho-1*, *let-502(sb106);rho-1(gf)* animals did not exhibit rescue of the *let-502(sb106)* defect (Table 2).

***mig-2* and *ced-10/rac-1* May Act in Parallel with *rho-1* During P Cell Migration.** Loss-of-function mutations in the Rac subfamily genes *mig-2* and *ced-10/rac-1* cause cell migration defects (10, 11). To

Table 2. P cell migration in *let-502, mig-2*, and *ced-10* strains

Genotype	Pn.p cells migrated‡	*n*
N2	11.0 ± 0.0	25
let-502(h392)	8.4 ± 1.1	25
let-502(sb106), 15°C	11.0 ± 0.0	20
let-502(sb106), 20°C	8.5 ± 1.5	20
let-502(RNAi)	8.5 ± 1.4	20
let-502(sb106);Ex rho-1(G14Vgf)	8.5 ± 1.5	20
Ex col-10:ced-10 (T17N, dn)	11.0 ± 0.0	25
ced-10(n3246)	11.0 ± 0.0	25
mig-2(mu28)	11.0 ± 0.0	25
ced-10(n3246); mig-2(RNAi)	9.0 ± 1.3	10
unc-73(e936)	7.6 ± 1.1	25
mig-2(mu28); unc-73(e936)	4.8 ± 1.1*	20
mig-2(mu28); unc-73(e936), Ex rho-1 (G14V, gf)	6.7 ± 1.1*	10
mig-2(gm103, gf)	7.0 ± 0.7†	25
mig-2(gm103, gf); Ex *rho-1(G14V, gf)*	9.3 ± 1.6†	25

Pn.p cells were scored during the L2 stage. Ex, extrachromosomal array. *ced-10* is also known as *rac-1*.

*, †, *P* value is <0.0001 when these data are compared by using Student's *t* test.

‡Data are expressed as the average number of Pn.p cells in the ventral cord during L2.

determine whether mutations in these genes affected the P cell lineage, we examined P cell migrations in *mig-2(mu28)* and *ced-10/rac-1(n3246)*, which are null and loss-of-function alleles, respectively. P cell migrations were normal in both *mig-2(mu28)* and *ced-10/rac-1 (n3246)* animals (ref. 10; Table 2). However, a weak P cell migration defect was observed in *ced-10/rac-1(n3246); mig-2(RNAi)* animals (Table 2). *ced-10/rac-1(n3246); mig-2(RNAi)* animals were rather sick, with many individuals developing slowly or not surviving past the second larval stage (data not shown; M. Sundaram, personal communication). The relatively low penetrance of the P cell migration phenotype could be because only relatively healthier animals lived long enough to be scored and a significant portion of the signal is through *rho-1*. The role of *mig-2* in P cell migration is also suggested by the observation that *mig-2(mu28)* exacerbates the weak P cell migration defect observed in *unc-73(e936)* (Table 2; ref. 10). This effect was weakly rescued by over expression of *rho-1(gf)* (Table 2). A gain-of-function mutation, *mig-2(gm103)*, results in weak P cell migration defects that are also partially rescued by *rho-1(gf)*. These observations support the hypothesis that parallel signaling of Rho family GTPases occurs during P cell migration (10).

Discussion

The proposal that *rho-1* is plays a role during P cell migration is based on the migration defect caused by *rho-1(dn)*, expression of the *rho-1* inhibitor C3, and *rho-1(RNAi)*. The *rho-1* (T19N) dominant-negative mutation is based on the homologous Ras (T17N) dominant-negative mutation and has been used to inhibit *rho-1* activity in many experimental systems (33, 34). Expression of the C3 enzyme specifically inactivates RHOA by ADP ribosylation at asparagine 41 (26). Our results identify RHO-1 as an important GTPase during P cell migration in *C. elegans*.

In addition to the P cell migration defects caused in *rho-1*-deficient animals, we observed gross morphological changes in ventral cord neurons. This effect appeared to be caused by inhibition of *rho-1* activity, because both *rho-1(dn)* animals and *rho-1(RNAi)* escapers displayed a similar phenotype. Staining with the DNA dye DAPI suggested the phenotype may be the result of failed cytokinesis, as many such cells were multinucleate. Multinucleate cells were also observed in early *rho-1(RNAi)* embryos (ref. 23; this study). These observations suggest that *rho-1* is required for at least some cytokinesis events in *C. elegans*. A role for *rho-1* in cytokinesis has also been reported in other organisms (35–37).

We also present results that are consistent with the idea that *unc-73* is an exchange factor for *rho-1* during P cell migration. Biochemical analysis of the UNC-73 exchange factor domains indicates that the GEF2 domain can efficiently catalyze GDP release from mammalian RhoA. It is reasonable to draw biochemical parallels between RHO-1 and RHOA because they share 85% primary structure identity including 98% identity in the GEF interaction domain (38, 39). Such biochemical parallels have been used to confirm genetic evidence in *C. elegans* previously (7). Genetically, mutations in both *unc-73* and *rho-1* cause a P cell migration defect, and a *rho-1(G14Vgf)* transgene can partially suppress the P cell migration defect in an *unc-73* mutant. These biochemical and genetic data, although subject to other interpretations, are consistent with a model in which *unc-73* and *rho-1* act together during P cell migration.

The G14V mutation is known to result in some constitutive activity of the RHO protein because of reduced intrinsic GTP hydrolysis (33). That rescue of the *unc-73(e936)* allele with *rho-1(gf)* was incomplete may be explained by two possibilities. First, the *rho-1(G14V)* mutation may not lead to a sufficiently strong hyperactive Rho protein. Rho family member proteins may need to cycle between GDP- and GTP-bound forms to achieve maximal activity. This has been proposed as an explanation for the observation that constitutively active Rho family members are only weak oncogenes (1), whereas endogenous RHO activated by exchange factors like Dbl can be potent (40, 41). It is also possible that Rho-1 may have a higher intrinsic GTPase activity that reduces the effectiveness of the G14V mutation. Second, as suggested by the results on *mig-2* and *ced-10/rac-1*, *unc-73* may function by activating more than one GTPase during P cell migration so that the *rho-1(gf)* gene can suppress only part of the defect associated with the *unc-73* allele.

There could also be several possible explanations for that the P cell migration phenotype in *unc-73* mutants are significantly weaker than that in the *rho-1(dn)* transgenic strain (Table 1). For example, it is possible that *rho-1* is activated by more than one exchange factor. In the Ras pathway in *C. elegans*, eliminating *let-341/SOS* function also results in a mutant phenotype that is significantly weaker than that of eliminating the *let-60/ras* function, promoting a proposal that there is another exchange factor for the Ras activation (42). Alternatively, the *unc-73(gm40)* mutants we examined may not eliminate enough *unc-73* activity. The severe sickness and lethality of the *gm40* mutant allowed us to examine only relatively healthy escapers among the homozygous progeny from heterozygous mothers. *gm40*, although a putative null from previous characterization (7), could be a non-null allele, and null mutations of the gene could be completely lethal at the embryonic or an early larval stage. Another possibility is that the RHO-1 GTPase activity may not totally depend on the activity from exchange factors. For example, repressing a Rho GDI (GDP-dissociation inhibitor) protein may also contribute to its activation (43). Therefore, *rho-1* may conceivably be partially active in absence of the UNC-73 function.

The idea of parallel GTPase signaling during P cell migration was first proposed after the observation was made that *mig-2(mu28, null)* exacerbates a P cell mislocalization phenotype of *unc-73(e936)* (10). Zipkin *et al.* speculated that *mig-2* is likely to act redundantly with another GTPase-dependent pathway during P cell nuclear migration. Our analysis of *rho-1*, *mig-2*, and *rac-1/ced-1* genes supports such prediction. A likely redundant role for *mig-2* and *ced-10/rac-1* in P cell migration is suggested by the observation that reducing the activity of both genes causes a defect in P cell migration, whereas single mutation in either gene does not (Table 2). Redundancy of these two gene activities

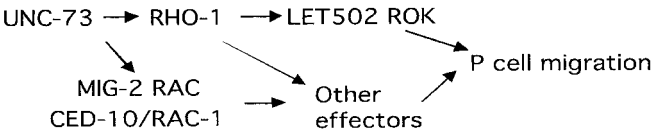

Fig. 5. Model for *rho-1*-mediated P cell migration.

has also been observed recently by others for axon guidance, cell migrations, apoptotic cell phagocytosis, and vulval morphogenesis (ref. 44; M. Sundaram, personal communication). We also confirmed that *mig-2(null)* exacerbates the phenotype of *unc-73(e936)* (Table 2) and show that such an effect is partially overcome by the *rho-1(gf)* transgene (Table 2). Thus, we may speculate that MIG-2 and CED-10/RAC-1 may act in parallel to RHO-1 and share UNC-73 as the exchange factor for the P cell migration function (Fig. 5). It is possible that the majority of the signal for P cell migration travels through the *rho-1* pathway because a more severe mutant phenotype is observed in the *rho-1(dn)* mutant and *rho-1(RNAi)* escapers. All proteins proposed to act during P cell migration in our model (Fig. 5) have been shown to express in the P cell lineage at the appropriate time (7, 10, 16, 45).

Our *in vitro* biochemical experiments also showed that UNC-73 GEF1 and GEF2 domains preferentially act on RAC and RHO proteins, respectively. Whether this preference is practiced *in vivo* in *C. elegans* is not clear. However, such a scenario has been previously indicated for UNC-73 homologues based on studies in mammalian cells (8, 9) and *Drosophila* (6).

Our interest in *let-502* was based on its homology to a known RHOA effector in mammals, p160ROCK (46). Because the *let-502* alleles examined can cause developmental arrest in the second or third larval stages, one must address whether development in these strains is generally impaired such that observations of various cell locations are subject to artifact. We do not believe that the observed P cell migration defects in *let-502* alleles are artifactual because the previously reported *let-502* defects appear to be restricted to embryonic elongation, and other markers of development appear to proceed normally (16). For example, the division and differentiation of P cell-derived GABA neurons marked by UNC-47::GFP appeared normal. In each *let-502* allele examined, a weak but reproducible P cell migration defect was observed. The *rho-1(gf)* transgene did not rescue the *let-502* P cell defect. Although LET-502 is likely an effector of RHO-1 during P cell migration, other effectors are likely to exist implicated by the weak P cell defect in *let-502*-deficient animals.

We are indebted to the labs of Rob Steven (University of Toronto), Joe Culotti (University of Toronto), Cynthia Kenyon (University of California, San Francisco), Erik Jorgensen (University of Utah), Paul Mains, Michinor Kohara, Yoshimi Takai, and Andy Fire for providing mutant strains and vectors. We also thank Rob Steven and Joe Culotti for discussion and comments on drafts of this manuscript and Lisa Williams from the Kenyon lab for suggestions on strain constructions. A.G.S. received support from a U.S. Army Breast Cancer Postdoctoral Fellowship (DAMD17–96-1–6041) and is currently a National Institutes of Health Postdoctoral Fellow (National Research Service Award HD8653). C.J.M was a National Defense Science and Engineering Graduate Fellow. This work was supported in part by National Institutes of Health Grant GM47869 (to M.H.). M.H. is an Assistant Investigator of the Howard Hughes Medical Institute.

1. Hall, A. (1998) *Science* **279,** 509–514.
2. Ridley, A. J. & Hall, A. (1992) *Cold Spring Harbor Symp. Quant. Biol.* **57,** 661–671.
3. Magie, C. R., Meyer, M. R., Gorsuch, M. S. & Parkhurst, S. M. (1999) *Development (Cambridge, U.K.)* **126,** 5353–5364.
4. Barrett, K., Leptin, M. & Settleman, J. (1997) *Cell* **91,** 905–915.
5. Prokopenko, S. N., Brumby, A., O'Keefe, L., Prior, L., He, Y., Saint, R. & Bellen, H. J. (1999) *Genes Dev.* **13,** 2301–2314.
6. Newsome, T. P., Schmidt, S., Dietzl, G., Keleman, K., Asling, B., Debant, A. & Dickson B. J. (2000) *Cell* **101,** 283–294.
7. Steven, R., Kubiseski, T. J., Zheng, H., Kulkarni, S., Mancillas, J., Ruiz-Morales, A., Hogue, C. W., Pawson, T. & Culotti J. (1998) *Cell* **92,** 785–795.
8. Debant, A., Serra-Pagès, C., Seipel, K., O'Brien, S., Tang, M., Park, S. H. & Streuli M. (1996) *Proc Natl. Acad. Sci. USA* **93,** 5466–5471.
9. Bellanger, J. M., Lazaro, J. B., Diriong, S., Fernandez, A., Lamb, N. & Debant, A. (1998) *Oncogene* **16,** 147–152.
10. Zipkin, I. D., Kindt, R. M. & Kenyon, C. J. (1997) *Cell* **90,** 883–894.
11. Reddien, P. W. & Horvitz, H. R. (2000) *Nat. Cell Biol.* **2,** 131–136.
12. Sulston, J. E. & Horvitz, H. R. (1977) *Dev. Biol.* **56,** 110–156.
13. Sulston, J. E. (1976) *Philos. Trans. R. Soc. Lond. Ser. B Biol. Sci.* **275,** 287–297.
14. Yochem, J., Gu, T. & Han, M. (1998) *Genetics* **149,** 1323–1334.
15. Piekny, A. J., Wissmann, A. & Mains, P. (2000) *Genetics* **156,** 1671–1689.
16. Wissmann, A., Ingles, J., McGhee, J. D. & Mains, P. E. (1997) *Genes Dev.* **11,** 409–422.
17. McIntire, S. L., Garriga, G., White, J., Jacbson, D. & Horvitz, H. R. (1992) *Neuron* **8,** 307–322.
18. McIntire, S. L., Reimer, R. J., Schuske, K., Edwards, R. H. & Jorgensen, E. M. (1997) *Nature (London)* **389,** 870–876.
19. Yochem, J., Tuck, S., Greenwald, I. & Han, M. (1999) *Development (Cambridge, U.K.)* **126,** 3597–3606.
20. Fire, A., Xu, S., Montgomery, M. K., Kostas, S. A., Driver, S. E. & Mello, C. C. (1998) *Nature (London)* **391,** 806–811.
21. Orita, S., Naito, A., Sakaguchi, G., Maeda, M., Igarashi, H., Sasaki, T. & Takai, Y. (1997) *J. Biol. Chem.* **272,** 16081–16084.
22. Orita, S., Kaibuchi, K., Kuroda, S., Shimizu, K., Nakanishi, H. & Takai, Y. (1993) *J. Biol. Chem.* **268,** 25542–25546.
23. Jantsch-Plunger, V., Gönczy, P., Romano, A., Schnabel, H., Hamill, D., Schnabel, R., Hyman, A. A. & Glotzer, M. (2000) *J. Cell. Biol.* **149,** 1391–1404.
24. Sulston, J. E. & Horvitz, H. R. (1981) *Dev. Biol.* **82,** 41–55.
25. Malone, C. J., Fixsen, W. D., Horvitz, H. R. & Han, M. (1999) *Development (Cambridge, U.K.)* **126,** 3171–3181.
26. Aktories, K. & Hall, A. (1989) *Trends Pharmacol. Sci.* **10,** 415–418.
27. Sieburth, D. S., Sundaram, M., Howard, R. M. & Han, M. (1999) *Genes Dev.* **13,** 2562–2569.
28. Grishok, A., Tabara, H. & Mello, C. C. (2000) *Science* **287,** 2494–2497.
29. Hedgecock, E. M., Culotti, J. G., Hall, D. H. & Stern, B. D. (1987) *Development (Cambridge, U.K.)* **100,** 365–382.
30. Chen, E. B., Branda, C. S. & Stern, M. J. (1997) *Dev. Biol.* **182,** 88–100.
31. Forrester, W. C. & Garriga, G. (1997) *Development (Cambridge, U.K.)* **124,** 1831–1843.
32. Habets, G. G., van der Kammen, R. A., Stam J. C., Michiels F. & Collard J. G. (1995) *Oncogene* **10,** 1371–1376.
33. Paterson, H. F., Self, A. J., Garrett, M. D., Just, I., Aktories, K. & Hall, A. (1990) *J. Cell Biol.* **111,** 1001–1007.
34. Sander, E. E., ten Klooster, J. P., van Delft, S., van der Kammen, R. A. & Collard, J. G. (1999) *J. Cell Biol.* **147,** 1009–1022.
35. Kishi, K., Sasaki, T., Kuroda, S., Itoh, T. & Takai, Y. (1993) *J. Cell Biol.* **120,** 1187–1195.
36. Mabuchi, I., Hamaguchi, Y., Fujimoto, H., Morii, N., Mishima, M. & Narumiya, S. (1993) *Zygote* **1,** 325–331.
37. Drechsel, D. N., Hyman, A. A., Hall, A. & Glotzer, M. (1997) *Curr. Biol.* **7,** 12–23.
38. Ihara, K., Muraguchi, S., Kato, M., Shimizu, T., Shirakawa, M., Kuroda, S., Kaibuchi, K. & Hakoshima, T. (1998) *J. Biol. Chem.* **273,** 9656–9666.
39. Li, R. & Zheng, Y. (1997) *J. Biol. Chem.* **272,** 4671–4679.
40. Srivastava, S. K., Wheelock, R. H., Aaronson, S. A. & Eva, A. (1986) *Proc. Natl. Acad. Sci. USA* **83,** 8868–8872.
41. Hart, M. J., Eva, A., Zangrilli, D., Aaronson, S. A., Evans, T., Cerione, R. A. & Zheng, Y. (1994) *J. Biol. Chem.* **269,** 62–65.
42. Chang, C., Hopper, N. A. & Sternberg, P. W. (2000) *EMBO J.* **19,** 3283–3294.
43. Van Aelst, L. & D'Souza-Schorey, C. (1997) *Genes Dev.* **11,** 2295–2322.
44. Lundquist, A. E., Reddien, P. W., Hartwieg, E., Horvitz, H. R. & Bargmann, C. I. (2001) *Development (Cambridge, U.K.)*, in press.
45. Chen, W. & Lim, L. (1994) *J. Biol. Chem.* **269,** 32394–32404.
46. Ishizaki, T., Naito, M., Fujisawa, K., Maekawa, M., Watanabe, N., Saito, Y. & Narumiya, S. (1997) *FEBS Lett.* **404,** 118–124.